scientific reports

Check for updates

OPEN

Prediction of cutting parameters and reduction of output parameters using machine learning in milling of Inconel 718 alloy

Maher Waleed Hamıd Hamıd[1], Barış Özlü[2]✉, Hasan Basri Ulaş[3] & Halil Demir[4]

The present study focuses on the effects of cooling/lubrication conditions and cutting parameters on energy consumption (EC), carbon emissions (CE), surface roughness (Ra), cutting temperature (T), tool wear (Vb) and vibration (Vib) in sustainable milling of Inconel 718 alloy. Also, it was aimed to estimate the EC, CE, Ra, T and Vib values obtained in milling experiments using three different regression-based machine learning (ML) models. The performances of the models used in ML were compared using R-squared, MSE and MAPE performance criteria. In the experiments conducted by reducing the feed rate and cutting speed and in MQL machining conditions, it was observed that EC and CE values reached minimum values. In MQL machining conditions, it was observed that the lowest Ra values were achieved at high cutting speed and low feed rate. The lowest Vb was measured at low cutting speed and feed rate in air machining conditions. Increasing the cutting speed and decreasing the feed rate in MQL machining conditions had a positive effect on Vib. In the MQL machining condition, at 40 m/min cutting speed and 0.06 mm/rev feed rate, the lowest energy consumption and carbon emission were 0.76 kJ/s and 0.54796 kg-CO_2 respectively. The lowest surface roughness and vibration values were measured as 0.234 µm and 1.91 mm/s respectively, at 80 m/min cutting speed and 0.06 mm/rev feed rate in MQL machining condition. The lowest cutting temperature was measured as 31 °C at a cutting speed of 40 m/min and a feed rate of 0.06 mm/rev under air machining conditions. It was seen that the EC, CE, Ra, T and Vib values arising from the input parameters in the machining of Inconel 718 alloy could be successfully predicted using three different regression-based ML models.

Keywords Energy consumption, Carbon emissions, Surface roughness, Cutting temperature, Tool wear, Vibration, Machine learning

Nickel-based superalloys have gained considerable popularity in aerospace, marine, chemical, refinery, automotive and many other industries due to their outstanding properties such as fatigue strength, corrosion and high temperature resistance[1,2]. In particular, the Inconel 718 alloy shows exceptional tensile strength and corrosion resistance while maintaining its mechanical properties at temperatures above 700 °C. Therefore, this alloy is widely used in petrochemical, nuclear and vehicle engineering as it meets the properties of parts operating at high temperatures, such as combustion chambers in the aviation industry[3]. Contrary to these properties, the high work hardening rate, low thermal conductivity, high strength, low material removal rate and the presence of carbide hard particles in its microstructure during processing put Inconel 718 alloy in the difficult-to-machine material class. As a result, during the machining of nickel-based superalloys, high cutting forces and cracks cause severe tool wear and deterioration of the surface integrity of the machined parts. These reasons reduce the overall performance and service life of superalloys where they are used[4–7].

Milling is one of the frequently preferred processing methods in the manufacturing industry for the production of parts in the requested size and shape, with precision and dimensional tolerances. This has made the milling technique one of the processing methods that attract the attention of researchers. In CNC milling, it is very important to achieve the desired result with low surface roughness, low tool wear, high material removal

[1]Department of Manufacturing Engineering, Institute of Graduate Education, Karabük University, Karabük 78050, Turkey. [2]Department of Mechanical Program, Aksaray University, Aksaray 68100, Turkey. [3]Department of Manufacturing Engineering, Gazi University, Ankara 06500, Turkey. [4]Department of Mechanical Engineering, Karabük University, Karabük 78050, Turkey. ✉email: barisozlu@aksaray.edu.tr

rate (MRR) and high production capacity and high efficiency. For this reason, researchers have preferred the CNC milling technique in examining the machinability performance of various materials in the industry[8,9].

In recent years, machine learning from artificial intelligence models has been used to model critical physical parameters and material performance in different systems[10–12]. Especially in the manufacturing sector, ML methods such as linear regression, support vector regression, decision tree classification, and Gaussian process regression are widely used to estimate and determine the optimum output parameters with processing parameters. Linear Regression provides simplicity and efficiency in modelling linear relationships and a solid starting point for tasks involving basic data structures. Support Vector Regression stands out with its ability to analyze nonlinear relationships thanks to its kernel functions and transform data into higher dimensional spaces to make these relationships linearly separable. SVR reduces prediction errors by maximizing the margin around a hyperplane and stands out as a suitable method for complex structures with this feature. Decision Tree Regression is one of the effective methods that divides data into similar subgroups based on decision rules. Its easy-to-understand structure and its capacity to represent nonlinear relationships make it a widely preferred option in foresight tasks[7,13].

When the studies on the machinability of Inconel 718 superalloy using turning and milling methods were examined in the literature, it was seen that studies were conducted on cutting tool coating[14,15], cutting tool geometry[16,17], high-speed machining[18,19], hot turning[20,21], minimum quantity of lubricant (MQL)[22,23], different cooling/lubrication techniques and sustainable machining[24–28]. It is seen that the studies conducted cover topics such as cutting force, surface roughness, cutting temperature, tool wear, energy consumption, carbon emissions and vibration analysis. Furthermore, it has been observed that studies are focusing on the effects and optimization of processing parameters on output parameters such as cutting force, surface roughness, tool wear, cutting temperature, energy consumption and carbon emissions[29–35]. The studies carried out focused on eliminating and improving the difficulties encountered in the processing of the difficult-to-machine Inconel 718 alloy, such as high cutting force, low surface quality, rapid tool wear, high cutting temperature, high energy consumption and carbon emission. In the literature, the studies are generally experimental. In addition to these, statistical methods such as the Finite Element Method (FEM), Regression, Artificial Neural Network (ANN), Adaptive Neuro-Fuzzy Inference System (ANFIS), Response Surface Methodology (RSM), Taguchi Method (TM), Genetic Algorithm (GA)[36,37] have been used for modelling and predicting inputs and outputs.

Climate change and environmental pollution have become increasingly dangerous for humanity. For this reason, especially in recent years, the importance of sustainability, reliability and carbon emission issues has increased in the manufacturing sector. Minimizing output parameters is of vital importance in the processing of Inconel 718 alloy, which is used in the production of critical parts such as engine and airframe components, nuclear applications, gas turbine ducts and combustion boxes in the manufacturing sector. Therefore, in the literature review, it was seen that the effects of cutting parameters and cooling/lubrication conditions on energy consumption, carbon emission, surface roughness, cutting temperature, tool wear and vibration in the machining of Inconel 718 alloy were investigated and the studies on the estimation of input and output parameters with ML methods were limited.

Therefore, this study aimed to investigate the effects of cutting parameters and cooling/lubrication conditions on energy consumption, carbon emission, surface roughness, cutting temperature, tool wear and vibration in the milling of Inconel 718 alloy. Additionally, energy consumption, carbon emission, surface roughness, cutting temperature and vibration were estimated using three different machine learning algorithms, namely linear regression, decision tree classifier, and support vector machines, and compared with experimental data. We believe that this study will contribute to the companies that produce using Inconel 718 alloy in the sector and to the researchers who will work on this alloy in the future.

Materials and methods

Workpiece material, cutting tool and machine tool

In the machining experiments, Inconel 718 alloy, commercially available from Bircelik Stainless Steel Trade Inc. in dimensions of $150 \times 30 \times 30$ mm, was used as the workpiece. The chemical composition of the alloy, as given by the company, is shown in Table 1. In the study, TiN/TiCN/Al_2O_3 coated carbide cutting tools in the KCPK30 quality group were used with the CVD method. Machining experiments were conducted on a CNC milling machine with 18.5 kW motor power and a maximum speed of 6000 rpm.

Cutting conditions

Machining experiments were conducted under three different cooling/lubrication conditions (dry, air and MQL). First, experiments were carried out in dry conditions for all cutting parameters. The second method is air cooling, in which the air-cooling system of the CNC machine, operating at a pressure of 6 bar, is used. A single nozzle was used in the cooling process. The cooling process was carried out by placing the nozzle at an angle of approximately 45° to the cutting area. Third, MQL cooling/lubrication method, in this method, Werte Mikro STN 15 model MQL system was used to deliver the cutting fluid to the machining area. MQL system has a 6 bar spray pressure and 0.028 ml/sec flow rate. Double nozzles with 2 mm diameter were delivered the cutting fluid to the machining area. Nozzles were positioned at a 45° angle to the cutting area. In the experiments, Mackerel

Materials	Ni	Co	Fe	Nb	Mo	Ti	Al	B	C	Mn	Si
Inconel 718	52.5	0.19	17.3	5.15	2.95	0.97	0.6	0.01	0.08	0.35	0.35

Table 1. Chemical composition of Inconel 718 alloy.

Feature	Unit	Explanation
pH		9.5
Intensity	15 °C, kg/m^3	1.070
Appearance	–	Clear-red brown
Smell	–	Typical
Yield point	°C, max	– 22
Refractive Index	n20/D	1.4222
Emulsion	5% demineralized water	Passe
Emulsion Stability	24	hours

Table 2. Technical specifications of Mackerel MS brand bio-stable semi-synthetic coolant.

Milling parameters	Symbols	Unit	Levels		
			Level 1	Level 2	Level 3
C/L condition	–	–	Dry	Air	MQL
Cutting speed	Vc	m/min	40	60	80
Feed rate	f	mm/rev	0.06	0.09	0.12

Table 3. Milling parameters and levels.

Ms brand bio-stable semi-synthetic metalworking fluid was used as the coolant. The properties of Mackerel Ms brand bio-stable semi-synthetic metalworking fluid are given in Table 2.

Experimental design

Cutting parameters (cutting speed, feed rate and depth of cut) and machining conditions (dry, air and MQL) in plane surface milling of Inconel 718 alloy were selected from the tool manufacturer's catalogue and based on previous studies in the literature. Taguchi's L27 orthogonal array, which includes three input factors and three levels of these factors given in Table 3, was used in the experimental design of these parameters. While the axial depth of cut was taken as 0.5 mm in the milling experiments, the axial depth of cut was determined as 1 mm in the tool wear experiments.

Measurement tools

Power consumption in the machining of Inconel 718 alloy was measured by connecting the clamps of the Lutron brand DW-6095-3 model phase power analyzer to the three-phase CNC machine. The average power consumption was calculated by averaging the data recorded by the device from the beginning to the end of the chip removal process. During the machining experiments, a FLIR İ60 brand infrared camera was used to measure the temperature in the cutting area. The temperature measurement range of the infrared camera used in the measurements is – 20 to 350 °C. The infrared camera was positioned at a distance of 250 mm from the cutting area and an angle of 45° during the measurements[38]. In each experimental combination, a Mitutoyo brand Surface SJ-210 model surface roughness profilometer was used to measure surface roughness. Vibration measurements were performed with the K333D01-VM digital vibration meter set. The vibration sensor was fixed on the workpiece with a screw. The vibration data obtained in each milling experiment was recorded using the VibeCheck program and the average vibration values were determined. To investigate the effect of cooling/lubrication environment and cutting parameters on tool wear in milling experiments, flank wear (Vb) was taken as 0.3 mm. After machining, tool wear measurements were performed with an Insize brand ISM-PM200SA model digital microscope. In addition, Scanning Electron Microscope (SEM) was used to visualize and examine the tool wear mechanisms in detail. The aim was to evaluate the effects of cooling/lubrication conditions and cutting parameters on carbon emissions during processing. For this purpose, carbon emission was calculated using Eqs. (1) and (2)[39].

$$E_{con} = \frac{Power \times Machining\ Time}{1000} \tag{1}$$

$$C_E = E_{con} \times Carbon\ emission\ indicator \tag{2}$$

It is defined as energy consumption (E_{con}) and carbon emission (C_E) given in Eqs. (1 and 2). In addition, the milling experiments and measurements experimental setup and details are given in Fig. 1.

Machine learning models

Linear regression

Linear regression (LR) is one of the simplest machine learning algorithms used in predictive solutions to a problem. This algorithm shows the linear relationship between a dependent variable and one or more independent variables. Therefore, it is called Linear Regression. The Linear Regression equation is given in Eq. (3)[40].

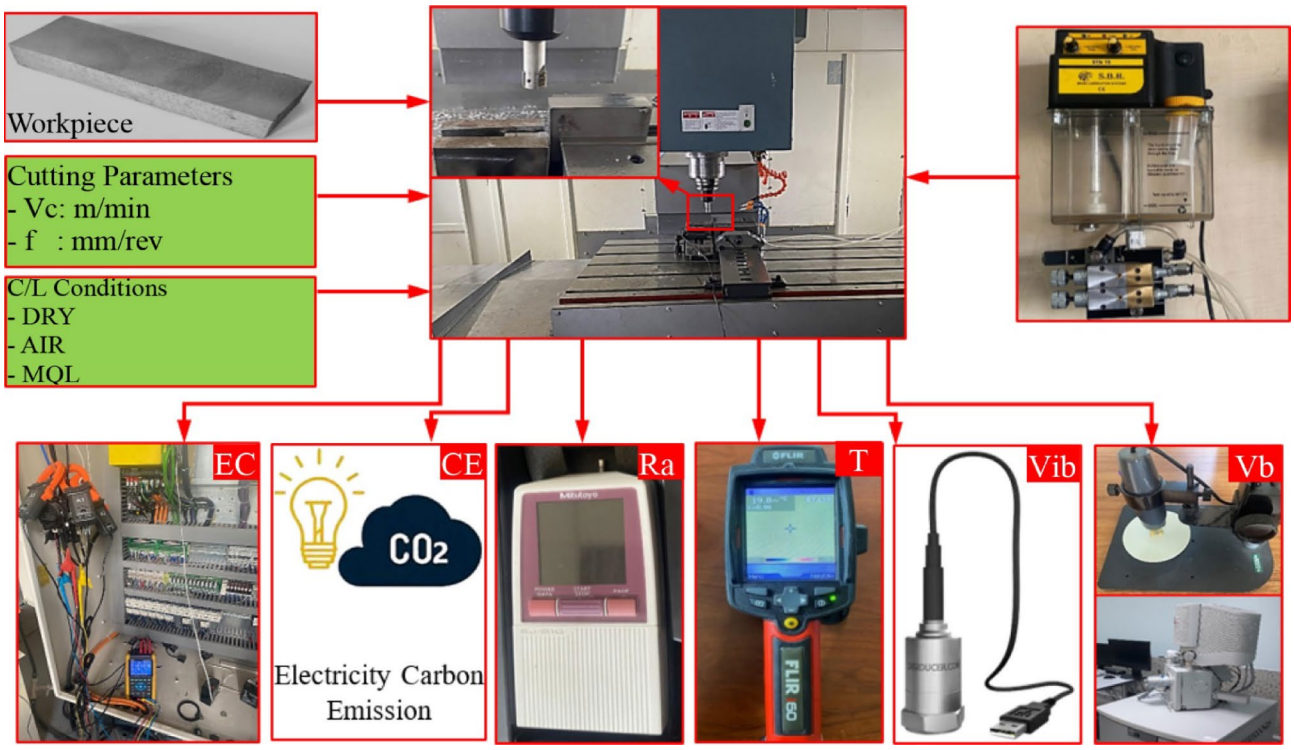


Fig. 1. Experimental setup used in the work.

$$Y = a_0 + a_1 X + \varepsilon \tag{3}$$

Equation (3) expresses the Y dependent variable, X independent variable, a_0 intercept of the line, a_1 linear regression coefficient and ε random error.

Decision tree classifier

Among supervised learning algorithms, one of the most used is tree-based learning algorithms. In general, it can be used to solve all the problems addressed. A decision tree is a classifier used to divide a data collection containing many records into smaller clusters by applying a series of decision rules. In other words, it is a structure used to divide large amounts of data into very small data groups by applying simple decision-making steps. The general structure of the Decision Tree Classifier (DTC) is given in Fig. 2.

Support vector machines

Support Vector Machine (SVM), proposed by Vapnik, is a supervised ML model mainly used for classification and at the same time, for prediction[24,25]. The goal of this algorithm is to obtain the best-fit line in a hyperplane with the maximum number of points, as shown in Fig. 3. The endpoints of SVM are selected to frame the hyperplane. These selected endpoints are given the name support vectors. In support vector regression, the distance between the boundary line and the hyperplane is the threshold value. SVM aims to fit the best line to the distance between the threshold values[26].

Model evaluation metrics

In this section, the trained models have been evaluated for performance. Three statistical criteria have been preferred to effectively evaluate the performance values of three different machine learning models. These are the mathematical expressions R-squared Error, in Equality 4, Mean Squared Error (MSE) in Equality 5, and Mean Absolute Percentage Error (MAPE) in Equality (6)[12,41], respectively.

$$R^2 = 1 - \frac{\sum_{i=1}^{n} \left(Y_i - \widehat{Y}\right)^2}{\sum_{i=1}^{n} \left(Y_i - \overline{Y}\right)^2} \tag{4}$$

$$MAPE = \frac{1}{n} \sum_{i=1}^{n} \frac{\left|Y_i - \widehat{Y}_i\right|}{Y_i} \times 100 \tag{5}$$

$$MSE = \frac{1}{n} \sum_{i=1}^{n} \left(Y_i - \widehat{Y}\right)^2 \tag{6}$$

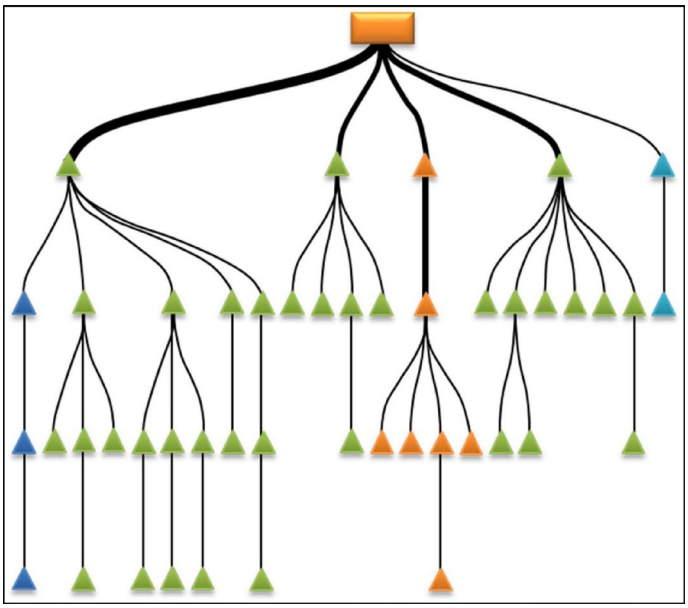


Fig. 2. The general structure of the decision tree classifier.

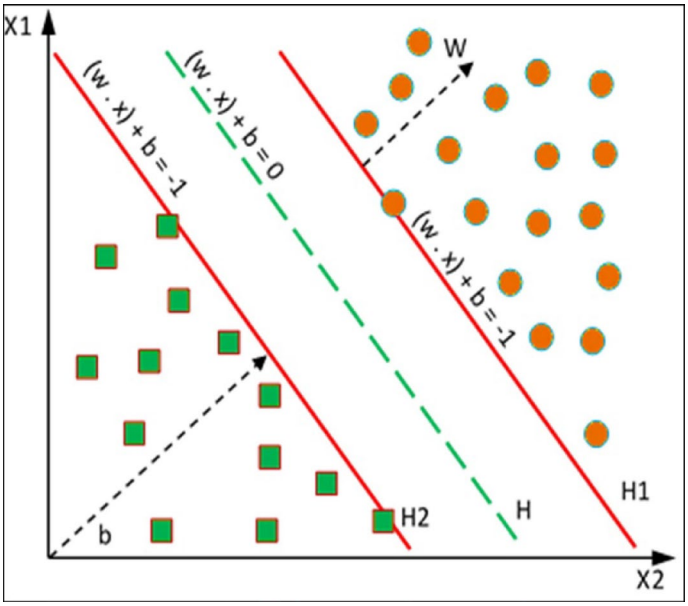


Fig. 3. Graphical representation of support vector machine.

In Eqs. (4–6), n represents the number of data points, Y_i represents the observed values, Y_i represents the predicted values and $\overline{Y}$ Y represents the mean value.

Results and discussion

Energy consumption

The milling of Inconel 718 alloy investigated the effects on energy consumption in cooling/lubrication conditions and cutting parameters. Figure 4 shows the differences in the energy consumption changes of cooling/lubrication conditions and cutting parameters in the milling of Inconel 718 alloy. As a result of the experiments, the energy consumption varies between 0.76 and 2.42 kJ/s. When Fig. 4 is examined, increasing the cutting speed and feed rate in all cooling/lubrication conditions caused an increase in energy consumption. In general, it has been observed that energy consumption increases with increasing cutting speed and feed rate under fixed cutting conditions. It has been reported that increasing the cutting speed will cause the spindle to rotate more, which will increase energy consumption[42,43]. When the effect of the feed rate on energy consumption was examined, it was determined that energy consumption increased parallel to the increase in the feed rate. Increasing the amount

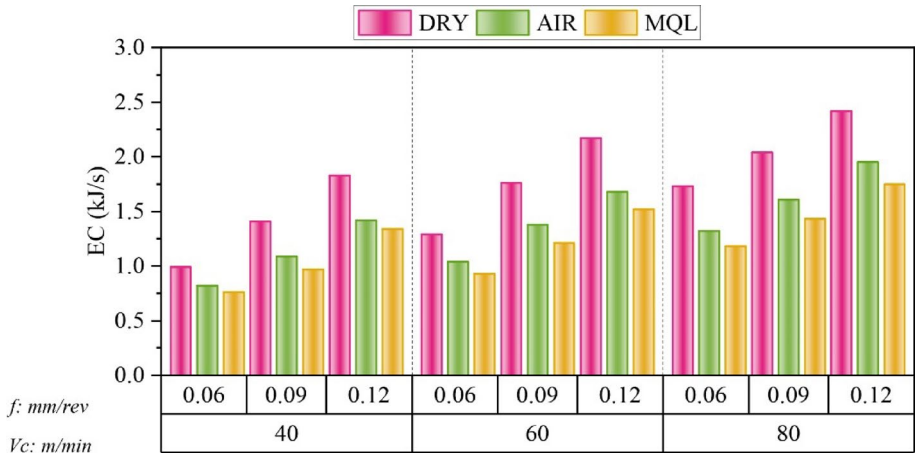


Fig. 4. Effects of the cooling/lubrication conditions and cutting parameters on the energy consumption.

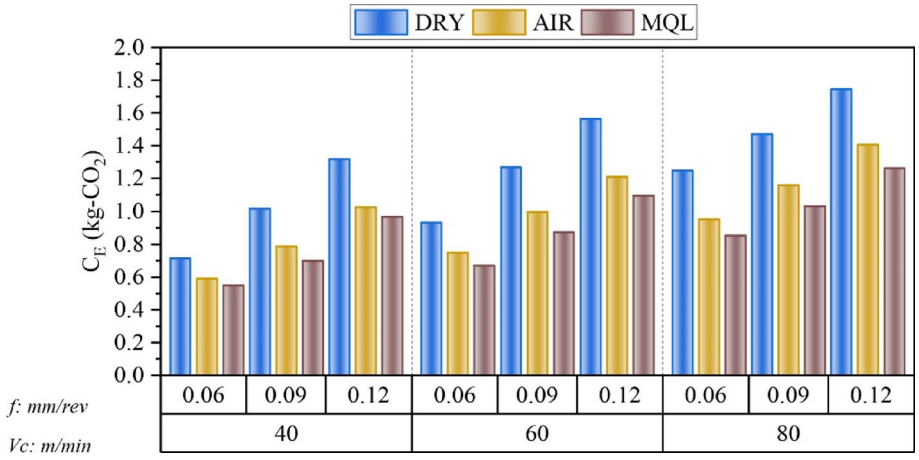


Fig. 5. Effects of the cooling/lubrication conditions and cutting parameters on the carbon emission.

of feed is a reason the axis motors move faster. It has been reported that the faster movement of the axis motors will also increase energy consumption[26,44].

In Fig. 4, at all cutting speed and feed rate values, cooling/lubrication conditions are seen to affect energy consumption. In general, energy consumption increased in the order DRY > AIR > MQL. Accordingly, it was observed that dry cutting conditions had the highest energy consumption and MQL machining conditions had the lowest. Researchers have reported that the oil employed in the MQL system diminishes the friction between the cutting tool and the workpiece, leading to a decrease in energy consumption[45]. Furthermore, it has been seen that tool wear in MQL machining conditions is less than in dry machining conditions. In this case, it has been reported that it reduces energy consumption. The more effective cooling with air compared to dry machining conditions delays tool wear. In this case, it has been reported that energy consumption in experiments carried out in air conditions has been reported less than in dry processing conditions[46,47].

Carbon emission

The effects of the carbon release of cooling/lubrication conditions and cutting parameters in the milling of Inconel 718 alloy are shown in the bar graph in Fig. 5. In Fig. 5, carbon emission values are seen between 0.54796 and 1.74482 kg-CO_2. At constant cooling/lubrication conditions, increasing the cutting speed and feed rate caused an increase in carbon emission values. In some previous studies, increasing the cutting speed has been reported to cause a decrease in cutting force and cutting power. It is also expected that carbon emissions will decrease parallel to the decreasing cutting force and cutting power[39,48,49]. However, in the study, under constant cutting conditions, increasing the cutting speed increased the machine spindle speed. Increasing the spindle speed caused the machine to draw more energy from the network. It is thought that the amount of carbon emissions will increase parallel with the increasing energy consumption. The increase in feed rate causes the tool-chip contact length to increase. Increasing the tool-chip contact length increased the cutting force, energy consumption and related carbon emission values. These results are shown parallel to previous studies in the literature[49–51].

The highest carbon emissions were produced with an average of 1.65 kg-CO_2 in the dry machining condition at constant cutting speed and feed rate. In the experiments carried out in the air and MQL processing conditions, carbon emission decreased by 17.23% and 25.43%, respectively, compared to the dry processing condition. Dry machining conditions have been identified as a method that minimizes machining costs, environmental pollution, and worker health problems by eliminating using coolants. Despite this definition, high energy consumption, production of high carbon emission amounts and poor part quality have been reported to limit sustainable processing under dry machining conditions[52]. In all cutting speed and feed rate combinations, the lowest carbon emission amount among cooling/lubrication conditions was obtained under the MQL machining conditions. This was followed by air and dry processing conditions, respectively. The reason for this, better penetration of MQL lubricant into the tool-workpiece interface creates an effective lubrication film[53]. It has been reported that the oil film formed at the tool-workpiece interface will reduce the cutting force by increasing cooling and reducing friction during machining[38]. Accordingly, energy consumption and carbon emissions are thought to decrease. It has been reported that the oil film reduces the cutting force by reducing the contact and adhesion tendency between the tool and chip[54]. In experiments conducted in air processing conditions, the amount of carbon emissions is lower than in dry processing conditions. In experiments conducted in air processing conditions, the amount of carbon emissions is lower than in dry processing conditions. Reduced tool wear causes the cutting tool to cut effectively. This will reduce the cutting force and energy consumption, therefore reducing the amount of carbon emissions.

Surface roughness

In this section of the article, the milling of Inconel 718 alloy has investigated the effects on surface roughness of different cooling/lubrication conditions and cutting parameters. Fig. 6 presents the effects of cooling/lubrication conditions and cutting parameters on the average surface roughness. As a result of the experiments, roughness values depending on cooling/lubrication conditions and cutting parameters have been observed to change between 0.214 and 0.987 µm. When Fig. 6 is examined, increasing the feed rate at constant cooling/lubrication conditions and cutting speed are the cause of a significant increase in surface roughness values. The feed rate is a function of surface roughness. Therefore, the negative effect of increasing feed rate values on surface roughness is a situation with its counterpart in the literature[25,55]. As the feed rate increases, the volume of chips removed per unit of time increases. This situation increases the forces generated during the cutting process and creates a more difficult cutting environment[56,57]. This situation is one of the factors that pave the way for an increase in surface roughness values. In addition, the increase in cutting force, tool wear and vibration with increasing feed rate is another factor that causes the roughness values to rise[4,40]. In the study, increasing the cutting speed caused the surface roughness to decrease. Surface roughness and cutting speed are inversely proportional. Low heat generation at the tool/chip interface at low cutting speeds does not reduce the hardness of the workpiece. This situation increases the cutting forces and loads on the tool, triggering tool wear. This causes the roughness values to be high. In addition, the BUE formed on the cutting tool at low cutting speeds has increased the roughness values. The BUE formed on the cutting tool throughout the cutting process increases and becomes indecisive. In the ongoing cutting process, BUE cannot withstand the stresses it is exposed to, so it breaks and separates from the cutting tool. It has been observed that the roughness values decrease by increasing the cutting speed from the lowest level to the highest level. The increase in cutting temperature parallel to the increasing cutting speed causes the workpiece to soften. This situation, causes the cutting process to be done more easily and decreases the surface roughness. Cutting force and vibration will decrease when machining a workpiece with reduced hardness. Previous studies have reported that reducing cutting forces and vibration has a positive effect on surface roughness[58,59].

When the effects of cooling/lubrication conditions on roughness values were examined, it was seen that the lowest roughness values were 0.363 µm on average in MQL machining conditions. Roughness values in air and dry machining conditions increased by an average of 47.4% and 94.5%, respectively, compared to MQL machining conditions. During machining, the lubrication of the cutting tool-workpiece by MQL caused the roughness values to be lower. It has been reported that the formation of a thin oil film layer by MQL in the cutting zone reduces friction and causes the roughness values to decrease[60]. Efficient lubrication will cause the chips formed during cutting to slide and move away from the tool surface more easily. This will lead to better surface quality during machining[61]. In experiments conducted in air processing conditions, the surface roughness value was found to be lower than in dry processing conditions. It is thought that providing low-temperature air to the cutting zone will cause the workpiece surface to solidify rapidly in a short time. This will eliminate the formation of irregular surfaces and reduce the roughness values. In dry machining conditions, the roughness values were higher than other cooling/lubrication conditions. In dry machining conditions, the cutting tool is in greater contact with the workpiece surface. In this process, the high cutting temperatures will increase tool wear. Increased tool wear causes surface roughness values to increase[62].

Cutting temperature

The temperature changes depending on the cooling/lubrication conditions and cutting parameters in the milling of nickel-based Inconel 718 superalloy are shown in Fig. 7. When Fig. 7 is examined, the cutting temperature values have been observed to change between 31 and 128 °C depending on the cooling/lubrication conditions and cutting parameters. It is seen that the cutting temperature increases significantly with increasing cutting speed at constant cooling/lubrication conditions and feed rate. It has been observed that the cutting temperature increases with the increase in feed rate at constant cooling/lubrication conditions and cutting speed. It is seen that increasing the cutting speed and feed rate in other cutting conditions causes the cutting temperature to rise. Two major problems cause the cutting temperature to increase in metal removal operations. Firstly, the low thermal conductivity of Inconel 718 (11 W/m°C) caused an increase in tool, chip and workpiece temperatures during

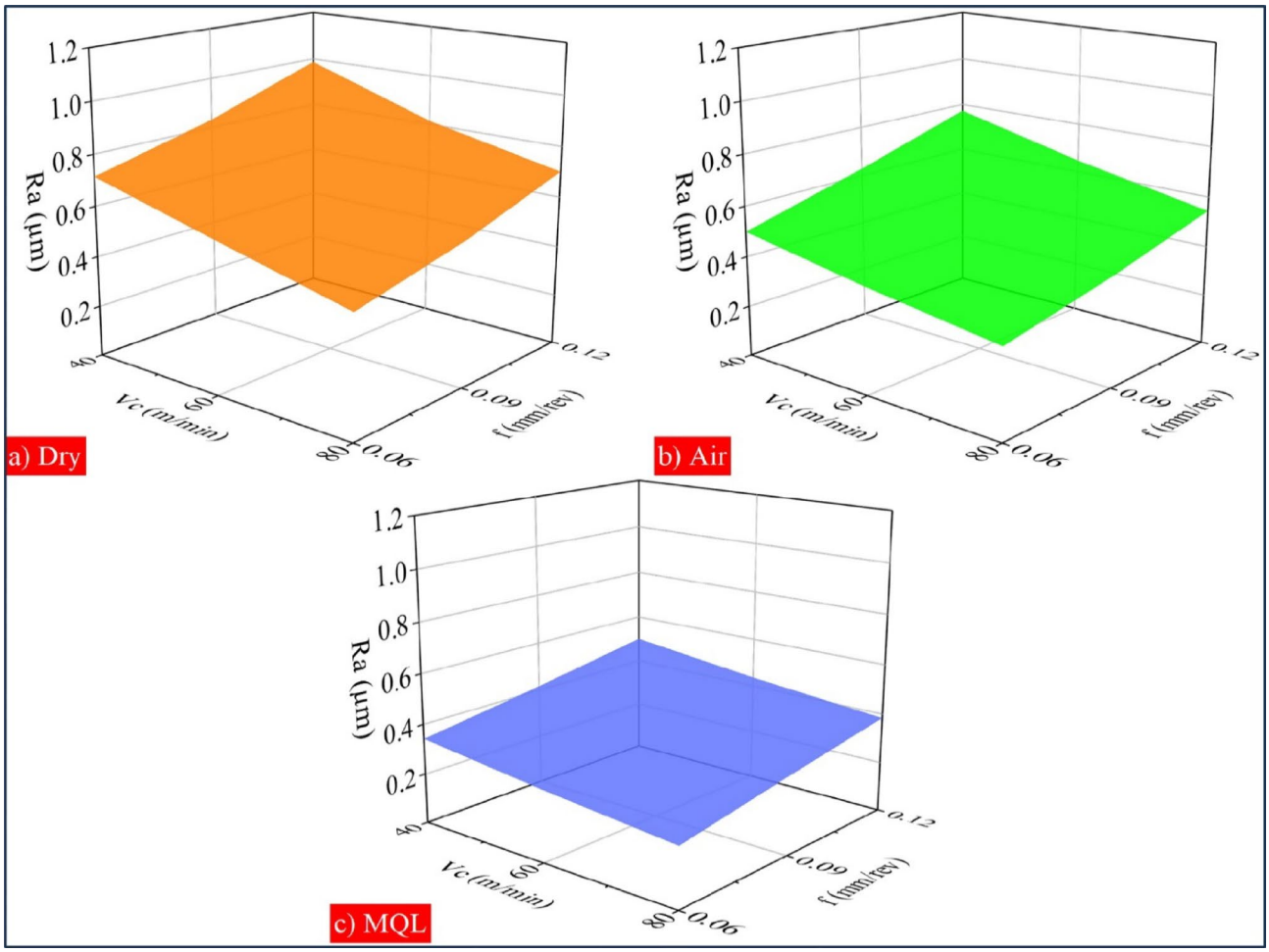


Fig. 6. Effects of the cooling/lubrication conditions and cutting parameters on the surface roughness.

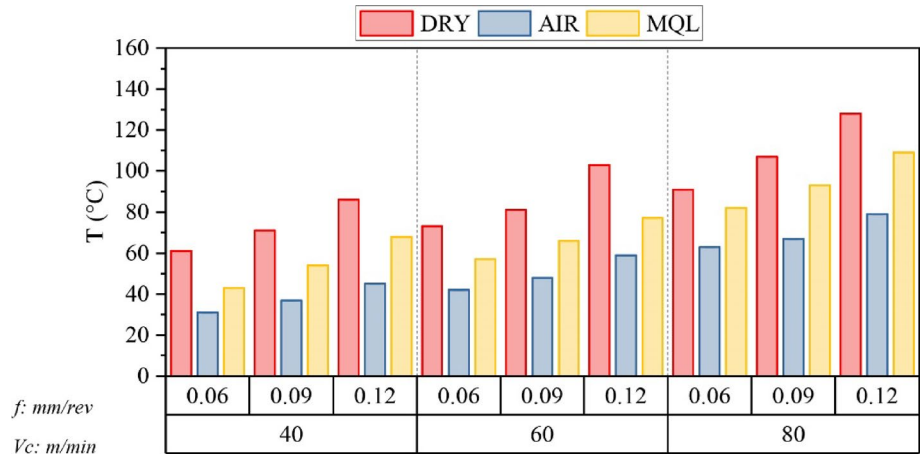


Fig. 7. Effects of the cooling/lubrication conditions and cutting parameters on the cutting temperature.

machining[63,64]. Secondly, the increase in cutting speed during machining increases the tool/chip contact time in unit time. The increased tool/chip contact time causes the friction to increase, thus the cutting temperature values[65]. These results in the study show parallelism to the literature. On the other hand, increasing the feed rate increases the amount of chips removed per unit of time, which increases the cutting temperature[66]. Constant cutting parameters were investigated effects on the cutting temperature of cooling/lubrication conditions. At a cutting speed of 40 m/min, a feed rate of 0.06 mm/rev and dry machining conditions, the cutting temperature

was measured as 61 °C. At constant cutting speed and feed rate, the cutting temperature decreased by 49.2% and 29.5% in air and MQL machining conditions. The maximum cutting temperature for all cutting parameters was measured under dry machining conditions. On the other hand, the lowest cutting temperature was measured in air machining conditions. The high-pressure air applied to the cutting zone effectively removes the chips formed during cutting. Furthermore, it is also thought that the thermal conductivity of air processing conditions is relatively lower than that of MQL processing conditions, which causes the cutting temperature to be low. In MQL machining conditions, the cutting temperature was lower than in dry machining conditions. Oil particles penetrate the tool/chip interface and form a thin film layer. The formed film layer causes the cutting temperature to decrease. In addition, the oil sprayed with MQL helps the chip to move away from the cutting zone[67].

Tool wear and damage mechanisms

The effects of cooling/lubrication conditions and cutting parameters on tool wear in the milling of Inconel 718 alloy were examined. In the experiments, the maximum tool wear (Vb) value was accepted as 0.3 mm. The changes in Vb values depending on the cooling/lubrication conditions and cutting parameters after the experiments are shown in Fig. 8. When Fig. 8 is examined, after approximately 30 min of cutting time, tool wear values are seen to vary between 0.052 and 0.395 mm. It has been observed that the cutting tool wears quickly with increasing cutting speed in all cutting conditions. The lowest tool wear was measured at the lowest cutting speed. The increase in heat generated at the tool-chip interface with the increase in cutting speed triggers the wear of the cutting tool. On the other hand, the increased volume of removed chips, along with the increased cutting speed, increases the friction between the tool and the workpiece. This situation affects tool wear in the negative direction[68]. Maximum tool wear was observed to occur under dry machining conditions and at all cutting speeds. Air by MQL machining conditions and all cutting speeds tool wear values have decreased significantly. It was observed that air and MQL machining conditions provided significant superiority in tool wear values compared to the dry machining condition. In MQL machining conditions, average tool wear values improved by 25.7% compared to dry machining conditions. The application of the oil used in MQL machining conditions to the tool/chip interface reduces friction and therefore, reduces the heat generated in the cutting zone. This situation contributed to the measurement of a higher tool life in the MQL machining condition according to the dry machining condition[69]. In air machining conditions, tool wear values were observed to improve by 46.7% and 28.3% compared to dry and MQL machining conditions. In the machining carried out at high air pressure, the formation of the lowest cutting temperature also had a positive effect on tool wear. On the other hand, it has been observed that the oil used in MQL machining conditions causes small chip particles to stick to the machined surface[70]. This situation increases the cutting temperature, which accelerates tool wear. In air processing conditions, small chip particles that may stick to the surface are removed from the cutting area with high air pressure. It is thought that removing small chip particles that may stick to the machined surface with high air pressure has a positive effect on tool wear by reducing the cutting temperature.

The effects of cooling/lubrication conditions and cutting parameters on tool wear types and wear mechanisms were investigated. For this purpose, SEM images and EDAX analyses taken from cutting tools are given in Fig. 9. When SEM images were examined, it was observed that tool wear types and wear mechanisms such as fracture region, coating removal, micro crack, built-up edge (BUE), built-up-layer (BUL), adhered work material, flank wear, and damaged cutting-edge line generally occur on cutting tools. In dry machining conditions, the absence of coolant/lubricant results in tool wear being distributed across a broad area. Upon examination of the surfaces of cutting tools employed under dry-cutting circumstances, fracture region is typically observed. In addition to this, coating removal, BUE, BUL and flank wear are observed on the cutting tool. It is known that the carbide particles in the structure of Inconel 718 superalloy cause abrasive wear in the first stage, which is caused by thermal and mechanical loads together with the chip[71]. As wear progresses, especially in the processing of superalloys, the adhesion of the workpiece to the cutting tool surface increases with increasing heat[72]. It reveals

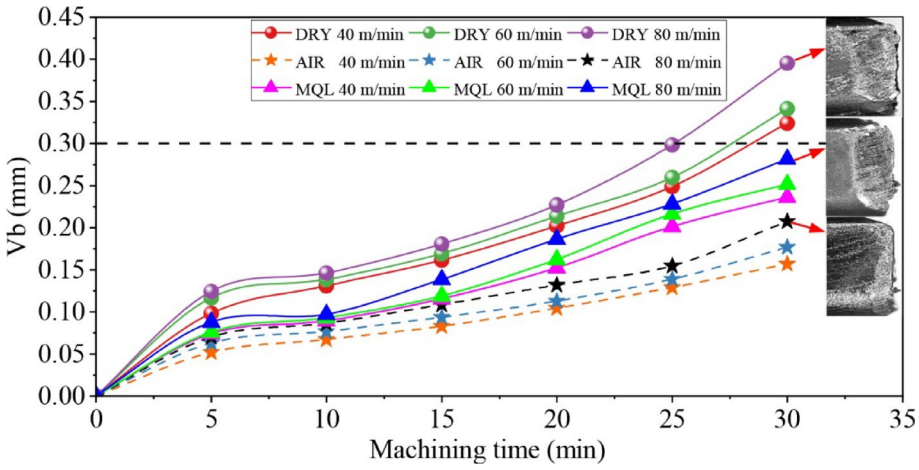
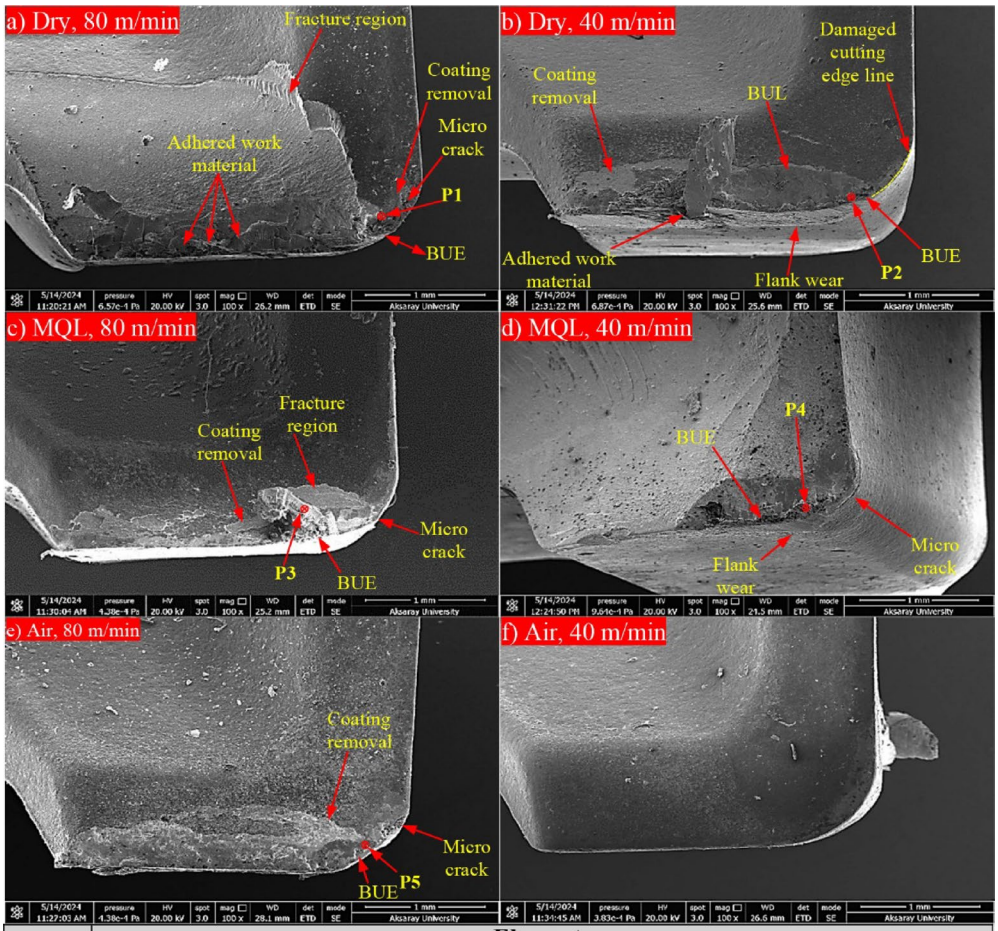


Fig. 8. The variation of flank wear with machining time for coolng/lubrication conditions and cutting parameters.



Points	Elements											
	B	C	Al	Si	Nb	Mo	Ti	Cr	Mn	Fe	Co	Ni
1	0.02	48.80	1.43	0.00	1.60	1.62	0.64	10.02	0.26	9.31	0.39	25.91
2	0.03	47.30	1.54	0.01	1.71	1.69	0.77	9.87	0.26	10.13	0.28	26.29
3	0.02	47.66	1.51	0.03	1.66	1.74	0.83	10.11	0.19	10.87	0.19	27.07
4	0.01	46.94	1.61	0.01	1.74	1.78	0.86	10.80	0.24	11.04	0.32	24.49
5	0,01	49.02	1.48	0.02	1.56	1.57	0.58	11.04	0.29	8.98	0.26	26.84

Fig. 9. SEM images and EDAX analysis results of worn tools under different cooling/lubrication conditions and cutting parameters have been conducted.

BUE and BUL formations, and the EDAX analysis also proves the results given in Fig. 9. BUE and BUL formed on the cutting tool cannot withstand the mechanical forces formed during the ongoing cutting period and move away from the cutting tool. This results in the development of wear types, including breakage, micro-cracking, chipping, and abrasion on the cutting tool[73]. It has been observed that the types of wear on the cutting tool decrease with the decrease in cutting temperature and friction in air and MQL machining conditions.

Vibration

The effects of cooling/lubrication conditions and cutting parameters on vibration are given in Fig. 10. When Fig. 10 is examined, it is seen that the vibration values, depending on cooling/lubrication conditions and cutting parameters, vary between 1.91 and 12.08 mm/s. Minimum vibration was measured as 1.91 mm/s in MQL machining conditions, at 80 m/min cutting speed and 0.06 mm/rev feed rate. Maximum vibration was measured as 21.08 mm/s in DRY machining conditions, at 40 m/min cutting speed and 0.12 mm/rev feed rate. As a result of the study, it was observed that increasing the feed rate and decreasing the cutting speed in all cooling/lubrication conditions had a negative effect on vibration. Increasing the feed rate causes the undeformed chip cross-section to increase. This increases the cutting forces and causes the vibration to be high. Increasing cutting forces cause the machine to be exposed to more load. This triggers more vibration in the bearings and bearings, causing higher vibration values. The increase in vibration in the machine leads to the deterioration of the surface quality of the workpiece. These results have been observed to be similar to many studies in the literature[74,75]. The decrease in vibration due to the increase in cutting speed and the rise in cutting temperature with the increase in cutting speed decreases the yield strength of the processed material and causes a decrease in cutting forces. As a result of this, the reduction in cutting forces is anticipated, as chip formation will occur more readily[76,77].

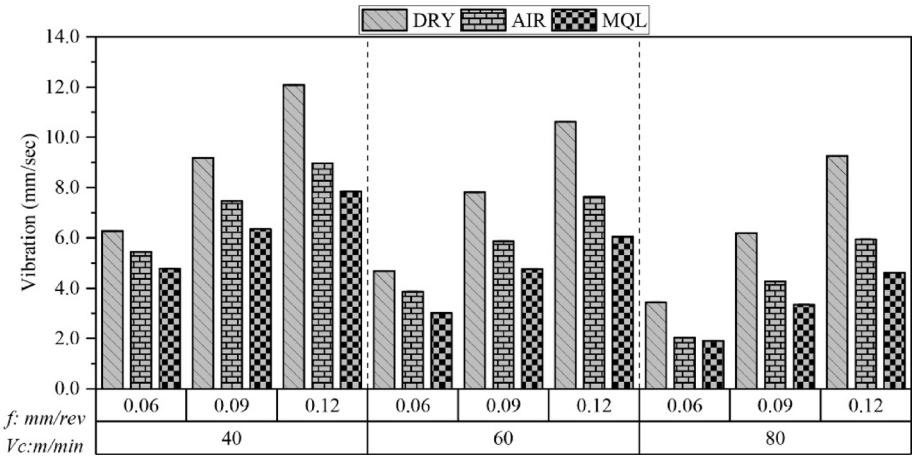


Fig. 10. Effects of the cooling/lubrication conditions and cutting parameters on the vibration.

It has been observed that the vibration will decrease with the decrease in the cutting forces and the load on the machine tool, which is in accordance with the studies in the literature[77,78]. When the effects of cooling/lubrication conditions on vibration were examined, the average vibration value in experiments conducted under dry machining conditions in all cutting parameters was 7.63 mm/s. It was observed that the vibration value decreased by 25.95% and 38.68% in air cooling and MQL lubrication conditions, respectively, compared to dry machining conditions. The oil used in MQL machining conditions creates an effective film layer between the tool and the workpiece. The formed film layer both protects the surface of the workpiece and reduces friction and vibration[79]. In addition, air and MQL processing conditions contribute to the reduction of heat values occurring in the cutting zone during processing. Thus, tool wear is reduced compared to the dry processing condition. It is thought that reduced tool wear will create a more regular cutting environment and cause a decrease in vibration.

Estimation of output parameters with machine learning

The energy consumption, carbon emission, surface roughness, cutting temperature and vibration values obtained in the milling experiments were estimated using three different regression-based machine-learning models (Linear Regression (LR), Decision Tree Classifier (DTC) and Support Vector Machines (SVM)). In creating the model of each output parameter, have been used a total of 27 data. Two-thirds of the input parameters were used for training and one-third for testing. These data were randomly selected. In estimating output parameters with different models has been selected three different cooling/lubrication conditions (DRY, AIR and MQL), three different cutting speeds and three different feed rates as input parameters. In order to minimize the errors that may occur due to the different units of the input parameters, a standard scalar was used in scaling the training and test data. The experimental values of energy consumption, carbon emission, surface roughness, cutting temperature and vibration obtained as a result of milling experiments and the estimated values obtained from LR, DTC and SVM are given in Table 4. The comparison of the experimental results with the estimated values obtained from LR, DTC and SVM is shown in Fig. 11. In addition, the performances of the models used in machine learning were compared using R-squared, MSE and MAPE performance criteria. In Table 5, the test errors obtained with R-squared, MSE and MAPE performance criteria for the estimated values obtained from LR, DTC and SVM are given.

Figure 11 shows the comparison of experimental values of energy consumption, carbon emissions, surface roughness, cutting temperature and vibration with the estimated values obtained with LR, DTC and SVM machine learning. When Fig. 11 is examined, it is seen that the SVM model provides a clear superiority over the LR and DTC models in estimating energy consumption, carbon emissions, surface roughness, cutting temperature and vibration. When the radar graphs are examined, it is seen that the experimental data of energy consumption, carbon emissions, surface roughness, cutting temperature and vibration are very close to each other with the values estimated by the SVM model. In this case, it is seen that the LR model makes predictions closer to the experimental data than the DTC model. In addition, the values obtained in the comparison of the performances of machine learning models with three different evaluation metrics are given in Table 5. When Table 5 is examined, it is seen that the accuracy is high in R-squared, MSE and MAPE performance evaluation as a result of the estimation of energy consumption, carbon emission, surface roughness, cutting temperature and vibration values with SVM, DTC and LR.

Conclusions

This paper focuses on the investigation of the effects of cooling/lubrication conditions and cutting parameters on energy consumption, carbon emissions, surface roughness, cutting temperature, tool wear and vibration in sustainable milling of Inconel 718 alloy. In addition, the energy consumption, carbon emission, surface roughness, cutting temperature and vibration values obtained in milling experiments were aimed to be estimated using three different regression-based machine learning models (Linear Regression (LR), Decision

Exp. Num	Exp. Value	Pre. SVM	Pre. DTC	Pre. LR	Exp. Value	Pre. SVM	Pre. DTC	Pre. LR	Exp. Value	Pre. SVM	Pre. DTC	Pre. LR
	PC				CE				Ra			
3	1.83	1.81	1.81	1.78	1.83	1.782	1.787	1.766	0.987	0.976	0.840	0.959
4	1.29	1.36	1.22	1.31	1.29	1.344	1.177	1.264	0.588	0.584	0.579	0.568
8	2.04	2.03	1.92	2.03	2.04	2.007	1.952	1.965	0.566	0.568	0.551	0.570
13	1.04	1.09	1.34	1.11	1.04	1.086	0.992	1.111	0.416	0.437	0.452	0.398
17	1.61	1.64	1.59	1.72	1.61	1.663	1.682	1.713	0.436	0.428	0.552	0.425
12	1.42	1.41	1.42	1.42	1.42	1.487	1.457	1.514	0.987	0.976	0.840	0.959
26	1.43	1.43	1.42	1.43	1.43	1.420	1.452	1.460	0.588	0.584	0.579	0.568
21	1.34	1.35	1.34	1.29	1.34	1.293	1.359	1.261	0.566	0.568	0.551	0.570
22	0.93	0.96	0.91	0.92	0.93	0.930	1.072	0.859	0.416	0.437	0.452	0.398
	T				Vib							
3	86.0	78.36	90.80	82.36	12.08	11.82	10.29	11.14				
4	73.00	73.00	71.38	72.89	4.69	4.98	4.54	5.48				
8	107.0	100.96	102.33	97.25	6.19	6.34	6.07	6.07				
13	42.0	39.16	39.38	41.39	3.86	3.72	4.61	3.99				
17	67.0	65.12	64.22	65.75	4.27	4.31	4.14	4.50				
12	45.0	45.52	50.60	44.86	8.97	9.25	7.62	9.66				
26	93.0	85.28	87.11	80.25	3.34	3.11	4.86	3.02				
21	68.0	67.68	69.80	66.36	7.84	7.52	6.43	8.17				
22	57.0	57.32	54.88	50.89	3.01	3.31	4.61	2.51				

Table 4. Experimental results obtained with three different regression-based machine learning models.

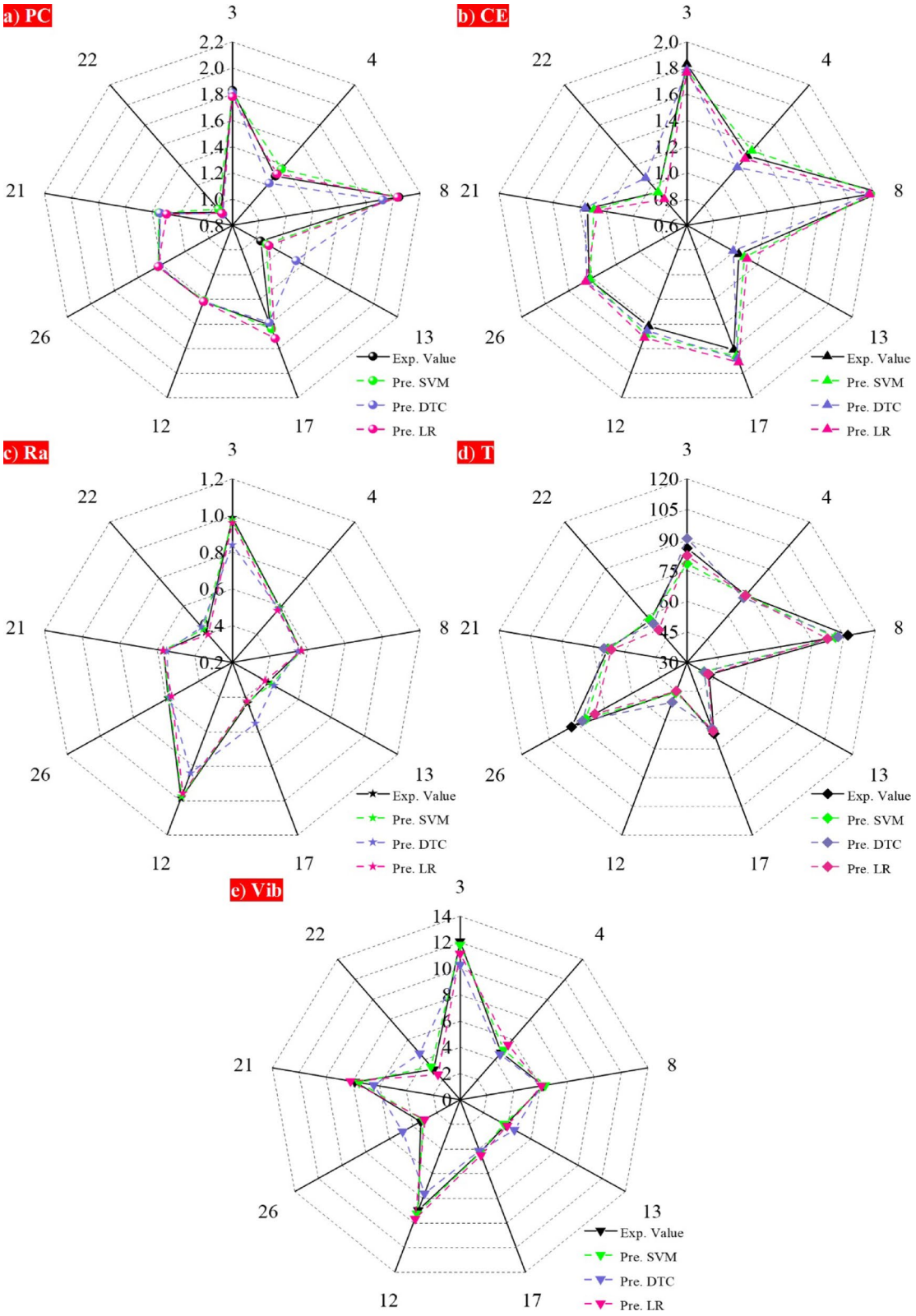


Fig. 11. Comparison of output parameters predicted using three different regression-based machine learning models.

Performance Indicator	R-squared	MSE	MAPE	R-squared	MSE	MAPE	R-squared	MSE	MAPE
	PC			CE			Ra		
SVM	0.94	0.0009	0.0189	0.9800	0.0020	0.0279	0.98	0.0001	0.028
DTC	0.81	0.0125	0.0508	0.9389	0.0058	0.0503	0.76	0.0088	0.157
LR	0.89	0.0025	0.0271	0.9517	0.0052	0.0496	0.96	0.0004	0.034
	T			Vib					
SVM	0.93	18.49	0.038	0.90	0.057	0.043			
DTC	0.80	15.09	0.053	0.76	1.386	0.193			
LR	0.88	34.75	0.048	0.88	0.281	0.081			

Table 5. Results of error percentage calculation of output parameters estimated using three different regression-based machine learning models.

Tree Classifier (DTC) and Support Vector Machines (SDM)). Some of the exciting results obtained from the study are summarized below:

- It has been observed that energy consumption and carbon emissions increase parallel to the increase in cutting speed and feed rate in the milling of Inconel 718 alloy under constant cooling/lubrication conditions. It has been observed that energy consumption and carbon emissions measured in MQL machining conditions decreased by an average of 29% compared to dry machining conditions in the milling of Inconel 718 alloy at constant cutting speed and feed rate.
- In the experiments, under constant cooling/lubrication conditions, the surface roughness tended to decrease with increasing cutting speed, while increasing the feed rate caused the surface roughness to increase. In the dry machining condition, the lowest surface roughness value was measured as 0.466 µm at 80 m/min cutting speed and 0.06 mm/rev feed rate. In air and MQL machining conditions with the same cutting parameters, the surface roughness decreased by 25.54% and 49.79%, respectively, compared to the dry machining condition.
- In the dry machining condition, the lowest cutting temperature was measured as 61 °C at 40 m/min cutting speed and 0.06 mm/rev feed rate. In the same cutting parameters, it was observed that the cutting temperature decreased by 49.18% and 29.51% in the air and MQL machining conditions, respectively, compared to the dry machining condition.
- In the experiments, under constant cooling/lubrication conditions, the surface roughness tended to decrease with increasing cutting speed, while increasing the feed rate caused the surface roughness to increase. In the dry machining condition, the lowest surface roughness value was measured as 0.466 µm at 80 m/min cutting speed and 0.06 mm/rev feed rate. In air and MQL machining conditions with the same cutting parameters, the surface roughness decreased by 25.54% and 49.79%, respectively, compared to the dry machining condition.
- It was observed that the maximum vibration value occurred at 12.08 mm/s at low cutting speeds, high feed rates and dry machining conditions. The vibration value decreased to the lowest level with 1.91 mm/s by increasing the cutting speed, decreasing the feed rate and in the MQL machining condition.
- The results of the study show that energy consumption, carbon emission, surface roughness, cutting temperature and vibration values arising from different cooling/lubrication conditions and different cutting parameters in the milling of Inconel 718 alloy can be successfully predicted using three different regression-based machine learning models (LR, DTC and SDM).
- In light of the study conducted, it is thought that the SVM model will provide advantages in terms of reducing time, cost, energy consumption, carbon emissions, labor and material losses by using Inconel 718 alloy in the production of parts by milling in the manufacturing industry.
- In addition, knowing the energy consumption, carbon emission, surface roughness, cutting temperature, tool wear and vibration of the Inconel 718 alloy according to the cooling/lubrication conditions and process parameters is of great importance for sustainable processing.
- In future studies on the milling of Inconel 718 alloy, different cutting tool coatings, different cutting tool geometry, different nanoparticle additions to MQL oil, different air pressures and cryogenic environments can be tried to minimize output parameters such as cutting force, energy consumption, carbon emissions, surface roughness. Different artificial intelligence models can be used to estimate input and output parameters.

Data availability

All data generated or analyzed during this study are included in this published article.

Received: 11 February 2025; Accepted: 26 May 2025
Published online: 26 September 2025

References

1. Aydin, K. Investigation of optimal machining Monel 400 superalloy considering carbon emissions using FEM, regression and ANN methods. *J. Clean Prod.* **447**, 141616. https://doi.org/10.1016/J.JCLEPRO.2024.141616 (2024).
2. Liu, Y. et al. Cutting performance and surface integrity for rotary ultrasonic elliptical milling of Inconel 718 with the ball end milling cutter. *J. Mater. Process. Technol.* **319**, 118094. https://doi.org/10.1016/J.JMATPROTEC.2023.118094 (2023).
3. Xu, M. et al. Machinability study of cryogenic-ultrasonic vibration-assisted milling Inconel 718 alloy. *Int. J. Adv. Manuf. Technol.* **127**, 4887–4901. https://doi.org/10.1007/S00170-023-11858-4/FIGURES/16 (2023).

4. Deshpande, Y., Andhare, A. & Sahu, N. K. Estimation of surface roughness using cutting parameters, force, sound, and vibration in turning of Inconel 718. *J. Braz. Soc. Mech. Sci. Eng.* **39**, 5087–5096. https://doi.org/10.1007/s40430-017-0819-4 (2017).
5. Ezugwu, E. O. et al. Evaluation of performance of various coolant grades when turning Ti–6Al–4V alloy with uncoated carbide tools under high-pressure coolant supplies. *J. Manuf. Sci. Eng.* **141**, 014503. https://doi.org/10.1115/1.4041778 (2019).
6. Kıvak, Ç. V. T. & Erzincanlı, F. Influence of different cooling methods on tool life, wear mechanisms and surface roughness in the milling of Nickel-based Waspaloy with WC tools. *Arab. J. Sci. Eng.* **44**, 7979–7995. https://doi.org/10.1007/S13369-019-03963-Y/TABLES/9 (2019).
7. Şap, S. et al. Machinability of different Cu–Gr composites in milling: Performance parameters prediction via machine learning models. *Expert Syst. Appl.* **272**, 126770. https://doi.org/10.1016/j.eswa.2025.126770 (2025).
8. Roy, S., Kumar, R., Panda, A. & Das, R. K. A brief review on machining of Inconel 718. *Mater. Today Proc.* **5**, 18664–18673. https://doi.org/10.1016/j.matpr.2018.06.212 (2018).
9. Kar, B. C., Panda, A., Kumar, R., Sahoo, A. K. & Mishra, R. R. Research trends in high-speed milling of metal alloys: A short review. *Mater. Today Proc.* **26**, 2657–2662. https://doi.org/10.1016/j.matpr.2020.02.559 (2020).
10. Zhang, Y. & Xu, X. Machine learning cutting force, surface roughness, and tool life in high-speed turning processes. *Manuf. Lett.* **29**, 84–89. https://doi.org/10.1016/j.mfglet.2021.07.005 (2021).
11. Özkan, E. K. & Ulaş, H. B. Comparison of four machine learning methods for occupational accidents based on national data on metal sector in Turkey. *Saf. Sci.* **174**, 106468. https://doi.org/10.1016/j.ssci.2024.106468 (2024).
12. Turan, İ, Özlü, B., Ulaş, H. B. & Demir, H. Prediction and modelling with taguchi, ANN and ANFIS of optimum machining parameters in drilling of Al 6082–T6 alloy. *J. Manuf. Mater. Process.* **9**, 92. https://doi.org/10.3390/jmmp9030092 (2025).
13. Jaypuria, S. et al. Prediction of electron beam weld quality from weld bead surface using clustering and support vector regression. *Expert Syst. Appl.* **211**, 118677. https://doi.org/10.1016/j.eswa.2022.118677 (2023).
14. Bhatt, A., Attia, H., Vargas, R. & Thomson, V. Wear mechanisms of WC coated and uncoated tools in finish turning of Inconel 718. *Tribol. Int.* **43**, 1113–1121. https://doi.org/10.1016/J.TRIBOINT.2009.12.053 (2010).
15. Zhou, J., Bushlya, V., Avdovic, P. & Ståhl, J. E. Study of surface quality in high-speed turning of Inconel 718 with uncoated and coated CBN tools. *Int. J. Adv. Manuf. Technol.* **58**, 141–151. https://doi.org/10.1007/S00170-011-3374-7/METRICS (2012).
16. Aslantas, K. & Alatrushi, L. K. H. Experimental study on the effect of cutting tool geometry in micro-milling of Inconel 718. *Arab. J. Sci. Eng.* **46**, 2327–2342. https://doi.org/10.1007/S13369-020-05034-Z/FIGURES/17 (2021).
17. Zhang, H. J., Sun, C., Liua, M. & Gao, F. Analysis of the optimization of tool geometric parameters for milling of Inconel718. *IOP Conf. Ser. Mater. Sci. Eng.* **426**, 012030. https://doi.org/10.1088/1757-899X/423/1/012030 (2018).
18. Ma, J. W., Wang, F. J., Jia, Z. Y. & Gao, Y. Y. Machining parameter optimization in high-speed milling for Inconel 718 curved surface. *Mater. Manuf. Process.* **31**, 1692e9. https://doi.org/10.1080/10426914.2015.1117623 (2016).
19. Tu, L. et al. Tool wear characteristics analysis of cBN cutting tools in high-speed turning of Inconel 718. *Ceram. Int.* **49**, 635–658. https://doi.org/10.1016/J.CERAMINT.2022.09.034 (2023).
20. Parida, A. K. & Maity, K. Numerical and experimental analysis of specific cutting energy in hot turning of Inconel 718. *Measurement* **133**, 361–369. https://doi.org/10.1016/J.MEASUREMENT.2018.10.033 (2019).
21. Parida, A. K. & Maity, K. Comparison the machinability of Inconel 718, Inconel 625 and Monel 400 in hot turning operation. *Eng. Sci. Technol. Int. J.* **21**, 364–370. https://doi.org/10.1016/J.JESTCH.2018.03.018 (2018).
22. Darshan, C. et al. Influence of dry and solid lubricant-assisted MQL cooling conditions on the machinability of Inconel 718 alloy with textured tool. *Int. J. Adv. Manuf. Technol.* **105**, 1835–1849. https://doi.org/10.1007/S00170-019-04221-Z/FIGURES/11 (2019).
23. Saleem, M. Q. & Mehmood, A. Eco-friendly precision turning of superalloy Inconel 718 using MQL based vegetable oils: Tool wear and surface integrity evaluation. *J. Manuf. Process.* **73**, 112–127. https://doi.org/10.1016/J.JMAPRO.2021.10.059 (2022).
24. Şap, E. et al. Understanding the effects of machinability properties of Incoloy 800 superalloy under different machining conditions using artificial intelligence methods. *Mater. Today Commun.* **38**, 108521. https://doi.org/10.1016/j.mtcomm.2024.108521 (2024).
25. Khanna, N., Airao, J., Kshitij, G., Nirala, C. K. & Hegab, H. Sustainability analysis of new hybrid cooling/lubrication strategies during machining Ti6Al4V and Inconel 718 alloys. *Sustain. Mater. Technol.* **36**, e00606. https://doi.org/10.1016/J.SUSMAT.2023.E00606 (2023).
26. Salur, E., Kuntoğlu, M., Aslan, A. & Pimenov, D. Y. The effects of MQL and dry environments on tool wear, cutting temperature, and power consumption during end milling of AISI 1040 steel. *Metals* **11**, 1674. https://doi.org/10.3390/MET11111674 (2021).
27. Tiwari, P. K., Raj, S., Kumar, R., Panda, A. & Sahoo, A. K. Machinability improvement investigation in face milling of Ti–3Al–2.5 V alloys using TiAlN coated carbide insert under dual nozzle minimum quantity lubrication cooling environment. *Proc. Inst. Mech. Eng. Part E J. Process. Mech. Eng.* https://doi.org/10.1177/09544089221132449 (2022).
28. Mallick, R., Kumar, R., Panda, A. & Sahoo, A. K. Current status of hard turning in manufacturing: Aspects of cooling strategy and sustainability. *Lubricants* **11**, 108. https://doi.org/10.3390/lubricants11030108 (2023).
29. Mallick, R. et al. Assessing hard-turning performance improvement using ionic liquid-infused cutting fluids: Tribological benefits, tool life assessment, and sustainable machining. *Proc. Inst. Mech. Eng. Part C J. Mech.* https://doi.org/10.1177/09544062251323036 (2025).
30. Siddique, M. Z. et al. Parametric analysis of tool wear, surface roughness and energy consumption during turning of Inconel 718 under Dry, Wet and MQL conditions. *Machines* **11**, 1008. https://doi.org/10.3390/MACHINES11111008 (2023).
31. Öztürk, B., Uğur, L. & Yildiz, A. Investigation of effect on energy consumption of surface roughness in X-axis and spindle servo motors in slot milling operation. *Measurement* **139**, 92–102. https://doi.org/10.1016/j.measurement.2019.02.009 (2019).
32. Özlü, B. Evaluation of energy consumption, cutting force, surface roughness and vibration in machining Toolox 44 steel using taguchi-based gray relational analysis. *Surf. Rev. Lett.* **29**, 2250103. https://doi.org/10.1142/S0218625X22501037 (2022).
33. Usca, Ü. A. et al. Estimation, optimization and analysis-based investigation of the energy consumption in machinability of ceramic-based metal matrix composite materials. *J. Mater. Res. Technol.* **17**, 2987–2998. https://doi.org/10.1016/j.jmrt.2022.02.055 (2022).
34. Şap, E., Usca, Ü. A., Değirmenci, Ü., Şap, S. & Uzun, M. Evaluation of machinability and energy consumption of CK45 steel using synthetic-based nanofluid and minimum quantity lubrication cutting fluid. *Metals* **15**, 36. https://doi.org/10.3390/met15010036 (2025).
35. Zerooğlu, T., Değirmenci, Ü. & Şap, S. A study on the machinability and environmental effects of milling AISI 5140 steel in sustainable cutting environments. *Machines* **12**, 436. https://doi.org/10.3390/machines12070436 (2024).
36. Al-Tamimi, A. A. & Sanjay, C. Intelligent systems to optimize and predict machining performance of inconel 825 alloy. *Metals* **13**, 375. https://doi.org/10.3390/MET13020375 (2023).
37. Yıldız, A., Uğur, L. & Parlak, İE. Optimization of the cutting parameters affecting the turning of AISI 52100 bearing steel using the Box-Behnken experimental design method. *Appl. Sci.* **13**, 3. https://doi.org/10.3390/app13010003 (2023).
38. Şirin, Ş & Kıvak, K. Effects of hybrid nanofluids on machining performance in MQL-milling of Inconel X-750 superalloy. *J. Manuf. Process.* **70**, 163–176. https://doi.org/10.1016/j.jmapro.2021.08.038 (2021).
39. Ross, N. S. et al. Carbon emissions and overall sustainability assessment in eco-friendly machining of Monel-400 alloy. *Sustain. Mater. Technol.* **37**, e00675. https://doi.org/10.1016/J.SUSMAT.2023.E00675 (2023).
40. Dubey, V., Sharma, A. K. & Pimenov, D. Y. Prediction of surface roughness using machine learning approach in MQL turning of AISI 304 steel by varying nanoparticle size in the cutting fluid. *Lubricants* **10**, 81. https://doi.org/10.3390/LUBRICANTS10050081 (2022).

41. Nguyen, A. T., Nguyen, V. H., Le, T. T. & Nguyen, N. T. Multiobjective optimization of surface roughness and tool wear in high-speed milling of AA6061 by machine learning and NSGA-II. *Adv. Mater. Sci. Eng.* **5406570**, 1–21. https://doi.org/10.1155/2022/5406570 (2022).
42. Akgün, M., Özlü, B. & Kara, F. Effect of PVD-TiN and CVD-Al_2O_3 coatings on cutting force, surface roughness, cutting power, and temperature in hard turning of AISI H13 steel. *J. Mater. Eng. Perform.* **32**, 1390–1401. https://doi.org/10.1007/S11665-022-07190-9/FIGURES/9 (2023).
43. Mahboob Ali, M. A., Azmi, A. I., Mohd Khalil, A. N. & Leong, K. W. Experimental study on minimal nanolubrication with surfactant in the turning of titanium alloys. *Int. J. Adv. Manuf. Technol.* **92**, 117–127. https://doi.org/10.1007/S00170-017-0133-4/METRICS (2017).
44. Suneesh, E. & Sivapragash, M. Parameter optimisation to combine low energy consumption with high surface integrity in turning Mg/Al_2O_3 hybrid composites under dry and MQL conditions. *J. Braz. Soc. Mech. Sci. Eng.* **41**, 1–23. https://doi.org/10.1007/S40430-019-1587-0/TABLES/20 (2019).
45. Sharma, A. K., Tiwari, A. K. & Dixit, A. R. Effects of minimum quantity lubrication (MQL) in machining processes using conventional and nanofluid based cutting fluids: A comprehensive review. *J. Clean. Prod.* **127**, 1–18. https://doi.org/10.1016/j.jclepro.2016.03.146 (2016).
46. Ul Haq, M. A. et al. Evaluating the effects of nano-fluids based MQL milling of IN718 associated to sustainable productions. *J. Clean. Prod.* **310**, 127463. https://doi.org/10.1016/j.jclepro.2021.127463 (2021).
47. Race, A. et al. Environmentally sustainable cooling strategies in milling of SA516: Effects on surface integrity of dry, flood and MQL machining. *J. Clean Prod.* **288**, 125580. https://doi.org/10.1016/J.JCLEPRO.2020.125580 (2021).
48. Khan, A. M. et al. Development of process performance simulator (PPS) and parametric optimization for sustainable machining considering carbon emission, cost and energy aspects. *Renew. Sustain. Energy Rev.* **139**, 110738. https://doi.org/10.1016/J.RSER.2021.110738 (2021).
49. Li, C., Tang, Y., Cui, L. & Li, P. A quantitative approach to analyze carbon emissions of CNC-based machining systems. *J. Intell. Manuf.* **26**, 911–922. https://doi.org/10.1007/S10845-013-0812-4/TABLES/9 (2015).
50. Sivalingam, V. et al. Towards sustainability assessment, energy consumption, and carbon emissions in cryogenic drilling of Alloy 20: A new approach towards sustainable future and challenges. *Int. J. Adv. Manuf. Technol.* **131**, 1151–1165. https://doi.org/10.1007/S00170-024-13144-3/FIGURES/15 (2024).
51. Zhang, H., Deng, Z., Fu, Y., Lv, L. & Yan, C. A process parameters optimization method of multi-pass dry milling for high efficiency, low energy and low carbon emissions. *J. Clean. Prod.* **148**, 174–184. https://doi.org/10.1016/j.jclepro.2017.01.077 (2017).
52. Gupta, M. K. et al. Environment and economic burden of sustainable cooling/lubrication methods in machining of Inconel-800. *J. Clean. Prod.* **287**, 125074. https://doi.org/10.1016/J.JCLEPRO.2020.125074 (2021).
53. Talib, N. & Rahim, E. A. Performance of modified jatropha oil in combination with hexagonal boron nitride particles as a bio-based lubricant for green machining. *Tribol. Int.* **118**, 89–104. https://doi.org/10.1016/j.triboint.2017.09.016 (2018).
54. Perçin, M., Aslantas, K., Ucun, I., Kaynak, Y. & Cicek, A. Micro-drilling of Ti–6Al–4V alloy: The effects of cooling/lubricating. *Int. J. Precis. Eng.* **45**, 450–462. https://doi.org/10.1016/j.precisioneng.2016.02.015 (2016).
55. Zahoor, S., Abdul-Kader, W., Shehzad, A. & Habib, M. S. Milling of Inconel 718: An experimental and integrated modeling approach for surface roughness. *Int. J. Adv. Manuf. Technol.* **120**, 1609–1624. https://doi.org/10.1007/s00170-021-08648-1 (2022).
56. Özlü, B., Demir, H., Türkmen, M. & Gündüz, S. Investigation of machinability of cooled microalloy stell in oil after the hot forging with coated and uncoated CBN cutting tools. *Sigma J. Eng. Nat. Sci.* **36**, 1165–1174 (2018).
57. Özlü, B. & Akgün, M. Evaluation of the machinability performance of PH 13–8 Mo maraging steel used in the aerospace industry. *Proc. Inst. Mech. Eng. Part E J. Process.* **238**, 687–699. https://doi.org/10.1177/09544089231216035 (2024).
58. Taha, Z. et al. Vortex tube air cooling: The effect on surface roughness and power consumption in dry turning. *Int. J. Automot. Mech. Eng.* **8**, 1477–1586. https://doi.org/10.15282/ijame.8.2013.34.0122 (2022).
59. Yıldırım, Ç. V., Kıvak, T., Sarıkaya, M. & Şirin, Ş. Evaluation of tool wear, surface roughness/topography and chip morphology when machining of Ni-based alloy 625 under MQL, cryogenic cooling and CryoMQL. *J. Mater. Res. Technol.* **9**, 2079–2092. https://doi.org/10.1016/j.jmrt.2019.12.069 (2020).
60. Şirin, Ş, Sarıkaya, M., Yıldırım, Ç. V. & Kıvak, T. Machinability performance of nickel alloy X-750 with SiAlON ceramic cutting tool under dry, MQL and hBN mixed nanofluid-MQL. *Tribol. Int.* **153**(106673), 2021. https://doi.org/10.1016/j.triboint.2020.106673 (2021).
61. Da Silva, L. R. et al. Analysis of surface integrity for minimum quantity lubricant-MQL in grinding. *Int. J. Mach. Tools Manuf.* **47**, 412–418. https://doi.org/10.1016/j.ijmachtools.2006.03.015 (2007).
62. Yalçın, B., Özgür, A. E. & Koru, M. The effects of various cooling strategies on surface roughness and tool wear during soft materials milling. *Mater. Des.* **30**, 896–899. https://doi.org/10.1016/j.matdes.2008.05.037 (2009).
63. Jafarian, F. et al. Finite element simulation of machining Inconel 718 alloy including microstructure changes. *Int. J. Mech. Sci.* **88**, 110–121. https://doi.org/10.1016/j.ijmecsci.2014.08.007 (2014).
64. Mahesh, K., Philip, J. T., Joshi, S. N. & Kuriachen, B. Machinability of Inconel 718: A critical review on the impact of cutting temperatures. *Mater. Manuf. Process.* **36**, 753–791. https://doi.org/10.1080/10426914.2020.1843671 (2021).
65. Kuzu, A. T., Berenji, K. R., Ekim, B. C. & Bakkal, M. The thermal modeling of deep-hole drilling process under MQL condition. *J. Manuf. Process.* **29**, 194–203. https://doi.org/10.1016/j.jmapro.2017.07.020 (2017).
66. Thakur, A., Gangopadhyay, S., Maity, K. P. & Sahoo, S. K. Evaluation on effectiveness of CVD and PVD coated tools during dry machining of incoloy 825. *Tribol. Trans.* **59**, 1048–1058. https://doi.org/10.1080/10402004.2015.1131350 (2016).
67. Khan, M. M. A., Mithu, M. A. H. & Dhar, N. R. Effects of minimum quantity lubrication on turning AISI 9310 alloy steel using vegetable oil-based cutting fluid. *J. Mater. Process. Technol.* **209**, 5573–5583. https://doi.org/10.1016/j.jmatprotec.2009.05.014 (2009).
68. Naves, V. T. G., Da Silva, M. B. & Da Silva, F. J. Evaluation of the effect of application of cutting fluid at high pressure on tool wear during turning operation of AISI 316 austenitic stainless steel. *Wear* **302**, 1201–1208. https://doi.org/10.1016/j.wear.2013.03.016 (2013).
69. Binali, R. Experimental and machine learning comparison for measurement the machinability of nickel based alloy in pursuit of sustainability. *Measurement* **236**, 115142. https://doi.org/10.1016/j.measurement.2024.115142 (2024).
70. Khaliq, W., Zhang, C., Jamil, M. & Khan, A. M. Tool wear, surface quality, and residual stresses analysis of micro-machined additive manufactured Ti-6Al-4V under dry and MQL conditions. *Tribol. Int.* **151**, 106408. https://doi.org/10.1016/j.triboint.2020.106408 (2020).
71. Salimi-Yasar, H., Heris, S. Z., Shanbedi, M., Amiri, A. & Kameli, A. Experimental investigation of thermal properties of cutting fluid using soluble oil-based TiO_2 nanofluid. *Powder Technol.* **310**, 213–220. https://doi.org/10.1016/j.powtec.2016.12.078 (2017).
72. Kaynak, Y., Gharibi, A. & Ozkutuk, M. Experimental and numerical study of chip formation in orthogonal cutting of Ti-5553 alloy: The influence of cryogenic, MQL, and high-pressure coolant supply. *Int. J. Adv. Manuf. Technol. Int.* **94**, 1411–1428. https://doi.org/10.1007/s00170-017-0904-y (2018).
73. Sani, A. S. A., AbdRahim, E., Sharif, S. & Sasahara, H. The influence of modified vegetable oils on tool failure mode and wear mechanisms when turning AISI 1045. *Tribol. Int.* **129**, 347–362. https://doi.org/10.1016/j.triboint.2018.08.038 (2019).
74. Asiltürk, I. & Akkuş, H. Determining the effect of cutting parameters on surface roughness in hard turning using the Taguchi method. *Measurement* **44**, 1697–1704. https://doi.org/10.1016/j.measurement.2011.07.003 (2011).

75. Hessainia, Z., Belbah, A., Yallese, M. A., Mabrouki, T. & Rigal, J. F. On the prediction of surface roughness in the hard turning based on cutting parameters and tool vibrations. *Measurement* **46**, 1671–1681. https://doi.org/10.1016/j.measurement.2012.12.016 (2013).
76. SreeramaReddy, T. V., Sornakumar, T., VenkataramaReddy, M. & Venkatram, R. Machinability of C45 steel with deep cryogenic treated tungsten carbide cutting tool inserts. *Int. J. Refract. Met. Hard Mater.* **27**, 181–185. https://doi.org/10.1016/j.ijrmhm.2008.04.007 (2009).
77. Benga, G. C. & Abrao, A. M. Turning of hardened 100Cr6 bearing steel with ceramic and PCBN cutting tools. *J. Mater. Process. Technol.* **143**, 237–241. https://doi.org/10.1016/S0924-0136(03)00346-7 (2003).
78. Bouacha, K., Yallese, M. A., Mabrouki, T. & Rigal, J. F. Statistical analysis of surface roughness and cutting forces using response surface methodology in hard turning of AISI 52100 bearing steel with CBN tool. *Int. J. Refract. Met. Hard Mater.* **28**, 349–361. https://doi.org/10.1016/j.ijrmhm.2009.11.011 (2010).
79. Carou, D., Rubio, E. M., Lauro, C. H. & Davim, J. P. The effect of minimum quantity lubrication in the intermittent turning of magnesium based on vibration signals. *Measurement* **94**, 338–343. https://doi.org/10.1016/j.measurement.2016.08.016 (2016).

Author contributions

M.W.H.H., B.Ö. and H.B.U. Conceptualization and methodology, M.W.H.H., B.Ö. and H.B.U. Conducting experiments, Validation of experiments, Writing-original draft, M.W.H.H., B.Ö., H.B.U. and H.D. Conducting analyses, Writing-original draft, Writing-review and editing, Resources, B.Ö., H.B.U. and Halil Demir, Writing-review and editing. All authors reviewed the manuscript.

Declarations

Competing interests

The authors declare no competing interests.

Additional information

Correspondence and requests for materials should be addressed to B.Ö.

Reprints and permissions information is available at www.nature.com/reprints.

Publisher's note Springer Nature remains neutral with regard to jurisdictional claims in published maps and institutional affiliations.

Open Access This article is licensed under a Creative Commons Attribution-NonCommercial-NoDerivatives 4.0 International License, which permits any non-commercial use, sharing, distribution and reproduction in any medium or format, as long as you give appropriate credit to the original author(s) and the source, provide a link to the Creative Commons licence, and indicate if you modified the licensed material. You do not have permission under this licence to share adapted material derived from this article or parts of it. The images or other third party material in this article are included in the article's Creative Commons licence, unless indicated otherwise in a credit line to the material. If material is not included in the article's Creative Commons licence and your intended use is not permitted by statutory regulation or exceeds the permitted use, you will need to obtain permission directly from the copyright holder. To view a copy of this licence, visit http://creativecommons.org/licenses/by-nc-nd/4.0/.

© The Author(s) 2025